TRG

CONTROL DATA CORPORATION

ON SONAR PERFORMANCE ESTIMATION FOR SEPARATED SOURCE AND RECEIVER

JUNE 1966

SUBMITTED TO:
NAVY ELECTRONICS LABORATORY
SAN DIEGO, CALIFORNIA

CONTRACT NO.:
NObsr-93023

REPORT NO.:
TRG-023-TM-66-23

TRG / A SUBSIDIARY OF CONTROL DATA CORPORATION
ROUTE 110 • MELVILLE, NEW YORK 11747 • 516/531-0600

LEVEL

WP11-2-41005

ON SONAR PERFORMANCE ESTIMATION FOR SEPARATED SOURCE AND RECEIVER,

by

R./Seegal and A./Novick

TRG Report No. 023-TM-66-23
Contract No. NObsr-93023

Submitted to:

U.S. Navy Electronics Laboratory
San Diego, California

Approved:

Walton Graham
Department Head, TRG

Approved:

Marvin Baldwin
Project Technical Director,
NEL

Isidore Cook
Deputy Project Technical
Director, DTMB

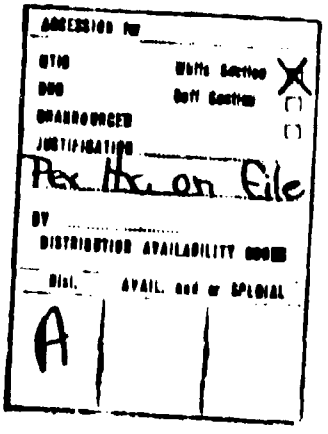

Submitted by:

TRG Incorporated
A Subsidiary of Control Data Corporation
Route 110
Melville, New York 11746

June 1966

CHANGE SHEET

CHANGE NUMBER	PAGE NUMBER	EFFECTIVE DATE

ABSTRACT

A model is developed for use in sonar performance prediction for systems using bistatic echo ranging. A mathematical model of the ocean, suited to performance calculations, is presented. The theoretical pattern for a rectangular array is developed from first principles, and the echo level and background level computations are outlined. This report is intended as a guide for future performance prediction work at TRG.

TABLE OF CONTENTS

LIST OF ILLUSTRATIONS

SECTION I

INTRODUCTION

This report covers the modeling phase of work done at TRG on the problem of performance estimation for a sonar system consisting of a physically separate source and receiver. This work is in the nature of an extension of the previous work in performance prediction for a coincident source and receiver. The goal of this study is to obtain an estimate of the potential sonar performance of systems with remote receivers for application to sonar systems design and application. A situation in which a sonar signal is received by a remote receiver can be useful enough to warrant consideration.

The concern of this study of sonar performance prediction in the bistatic case is the computation of the echo-to-background ratio (E/B) developed by a separated source and receiver system against a submarine target. Comparisons of the E/B obtained by various systems provide guidance in system design and application.

After a discussion of the motivations for a bistatic echo ranging study, this report will proceed by outlining the ocean model used in the systems calculations. Next, the echo-level calculations for bistatic situations will be discussed as an extension of the monostatic echo-level calculation (as already implemented at TRG). Finally, the estimation of boundary reverberation will be discussed in terms of a continuation of the techniques now used in monostatic reverberation. This report shows the direction in which sonar performance prediction for separated source and receiver at TRG is proceeding. (The monostatic calculations are set forth in 023-TM-66-16, a companion volume (Reference 24 of this report)).

MOTIVATION FOR THE BISTATIC-ECHO RANGING STUDY

The potential advantage of a sonar system with a remote receiver over a system with coincident source and receiver

is due to its added freedom in the placement of the receiver. This advantage is due not only to the potentially higher echo-to-background ratios obtainable, but also to the geometric situation which may allow a more precise determination of the target location. A sonar system restricted to monostatic echo ranging must be content with whatever propagation conditions exist between it and the target for both the transmission and reception paths. On the other hand, a bistatic system may take advantage of more favorable propagation conditions for the target-to-receiver path. When the receiver is positioned so that the reception path is direct, the target localization is essentially independent of the bottom roughness, which presents a problem for bottom bounce sonars. (In addition, multiple receivers may be used to pin-point the target.)

Furthermore, a system with a remote receiver may lead to more advantageous target localization than monostatic systems. With the position of the source and receiver known, the echo travel time determines a contour on which the target must lie. (The specification of this contour is discussed in Section VI.) To fix the target location uniquely, further information is needed. A bearing from the source (which also receives) could locate the target.

Alternatively, the receiver could also contain a transponder to take advantage of the Loreli target localization. (See Reference 30.) A Loreli-type system, with a remote receiver could localize the target as the intersection of the Loreli bearing with the contour determined by the echo travel time. (The Loreli bearing is found by subtracting the sonar vector from the source to the receiver/transponder from the sonar vector to the target, which is also detected monostatically.)

This subtraction serves to eliminate systematic errors (e.g. velocity gradients in the horizontal direction, or sonar alignment errors) from the target localization. As with Loreli systems, a sonar system with a remote receiver in the vicinity of the target converts the long-range fire control problem, requiring high absolute accuracy, to a short-range fire control problem, requiring only relative accuracy. The geometry is illustrated below in Figure 1-1.

Several studies have indicated the superiority of multistatic echo-ranging systems. (See, for example, Reference 31). Work in underwater target classification has shown that bistatic techniques produce more information than monostatic systems (because the echo structure depends on the bistatic angle (defined in Section V)). Current work in target classification is based on the use of multistatic systems which can provide the necessary information. Theoretical studies were verified by at-sea experiments in locating and classifying submarine targets, indicating the feasibility of multistatic systems in target classification. Furthermore, the tactics required for a multistatic classification position the elements of the ASW system so that they can maintain contact with a fast, maneuverable target.

In addition, studies and experience show that a multistatic system, because of its higher information rate, can classify a target in a shorter time than a monostatic system, although the multistatic geometry takes longer to set up . The multistatic system has further advantages. First, it receives more information on the target's speed and course due to the additional sensors in the geometry. Second, the tactical disbursement of the ASW system elements restricts the target escape capabilities.

In addition to studies based on multistatic echo ranging, bistatic situations are commonly encountered in cur-

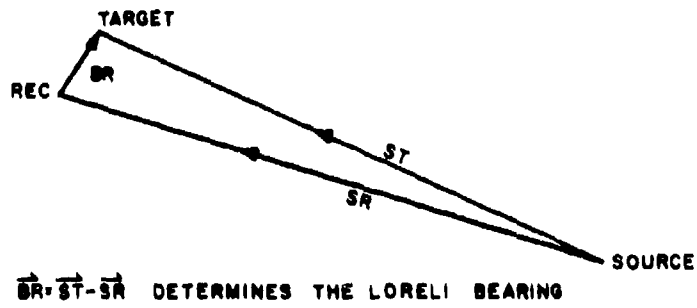

Figure 1-1. BISTATIC TARGET LOCATION GEOMETRY

rent tactical situations. Convoying operations offer an illustration of the effectiveness of a remote receiver system. Here, a number of escort vessels operate in the active mode. Monostatic operation restricts each ship to listen only to its own echo. An understanding of the bistatic problem would allow escort vessels to take advantage of the other's transmissions. The use of sonobuoys to receive active transmissions (from some other source) also involves a bistatic situation.

The above examples indicate the possible advantages of bistatic sonar systems implying a need for a performance prediction capability for bistatic sonars. Such a capability would provide guidance in system design and application. Familiarity with the bistatic problem would not only allow more tactical freedom in the use of sonars, but it would also shed light on the operational problem of mutual sonar interference. Optimal tactical positioning of sonar ships requires an investigation of the interference problem, involving the same calculations as the bistatic echo-ranging problem.

For system performance purposes, the general problem concerns the echo-to-background ratio for arbitrary placement of the source and receiver. The extension of present prediction capabilities to the bistatic case will allow an investigation of the effects of ship motion, including translation, roll, pitch, and yaw, on sonar performance, as a special case. (Different transmit and receive systems on the same ship could also be evaluated) Furthermore, the extension of the bistatic solution to the multistatic problem for sonobuoy arrays and multiple escort vessels configurations is straightforward. For the reasons outlined above, an investigation of bistatic echo ranging, from the point of view of performance prediction, is needed for a more complete understanding of the operations of complex, multi-element sonar system.

An understanding of the various bistatic sonar applications described above should lead to improved utilization

of current and planned sonar systems. In addition, a remote passive receiver will not alert a target to the fact that it has been detected; an unalerted target, coupled with improved localization should result in greatly improved weapon effectiveness. Finally, as a harassing tactic, the possible use of remote receivers would be an added threat for the submarine commander by restricting his use of good propagation paths, degrading his information and, hence, his performance.

SECTION II

GENERAL CONCEPTS

The fundamental concepts used in systems analysis are discussed in Section I of Reference 1. Some of the topics covered in this section are summarized below:

Directivity Index, DI:

$$DI(db) = 10 \log_{10} \frac{4\pi \times \text{Effective Area}}{(\text{Wavelength})^2}$$

Source Level, L_p

$$L_p(\text{db re 1 } \mu\text{bar at 1 yd}) = 101.6 + 10 \log_{10}[\text{Power Out(kw)}] + DI.$$

Noise Level, L_{epw}

If the noise is truly isotropic, the equivalent plane wave noise level, L_{epw}, is given by:

$$L_{epw}(\text{db re 1}\mu\text{bar}^2) = \text{Isotropic spectrum level (db re 1}\mu\text{bar}^2\text{/cps)} - DI + 10 \log_{10}[\text{bandwidth(cps)}]$$

If the noise is uncorrelated between elements*, e.g., flow induced noise, then L_{epw} is given by:

$$L_{epw} = \text{Single element spectrum level (db re 1}\mu\text{bar}^2\text{/cps)} - 10 \log_{10}(\text{no. of elements}) + 10 \log_{10}(\text{bandwidth})$$

Background Level, L_b

The background level is assumed to be composed of reverberation and noise. Since these background signals are uncorrelated, the total power is the sum of the powers of the signals.

*Over the range of time delays used for beamforming

Echo Level, L_e

The echo levels are computed from the standard echo ranging equation,

$$L_e(\text{db re } 1\mu\text{bar}^2) = L_p + N_{ts} - 2N_w - (\text{transmission + reception deviation loss}).$$

where: N_{ts} = target strength (in db).

N_w = two-way propagation loss (in db).

SECTION III

OCEAN MODEL

The basic ocean model assumed for the echo and reverberation level calculations is described in the following sections.

A. PROPAGATION

1. Propagation Loss

The propagation loss is given by the sum of the individual ray path losses; namely, propagation loss = spreading loss + reflection losses + absorption loss.

The spreading loss in an isovelocity medium given by 20 $\log_{10}$ (slant range). The calculation of spreading loss in a refractive medium is described below. The reflection processes are discussed below.

2. Absorption Loss

The absorption loss coefficient (db/kyd) is represented by a general power law equation; that is, the coefficient is equal to a constant times the frequency raised to some power. The absorption loss in db is given by the product of the coefficient and the slant range to the target (which is approximated by the mean sound velocity x travel time along the path).

3. Ray Tracing

The velocity profile is assumed to be a function of depth only, and is approximated by a series of layers, each with a constant velocity gradient. For a ray traversing a single layer, the basic formulas used for the ray tracing calculations are summarized below:

$$\Delta R = \frac{V_x}{g} (\sin \theta_e - \sin \theta_\ell) \qquad (1)$$

$$\frac{d\Delta R}{d\theta_o} = \frac{V_x \tan \theta_o}{g} \left(\frac{1}{\sin \theta_o} - \frac{1}{\sin \theta_\ell} \right) \quad (2)$$

$$\Delta T = \frac{1}{g} \log_e \frac{(1+\sin\theta_e)(1-\sin\theta_\ell)}{(1-\sin\theta_e)(1+\sin\theta_\ell)} \quad (3)$$

$$\frac{d\Delta T}{d\theta_o} = \frac{1}{V_x} \frac{d\Delta R}{d\theta_o} \quad (4)$$

where:

ΔR is the incremental horizontal range

θ_o is the inclination angle of the ray at the source depth,

θ_e is the inclination angle of the ray at its entry into the layer,

θ_ℓ is the inclination angle of the ray when it leaves the layer,

ΔT is the incremental travel time (in seconds) through the layer,

V_x is the Snell's law constant and is given by

$$V_x = \frac{V_o}{\cos\theta_o} \quad \text{where:}$$

V_o is the sound velocity at the source,

g is the velocity gradient in the layer and is given by:

$$g = \frac{V_\ell - V_e}{\Delta d} \text{, where:}$$

V_e is the velocity of sound at the depth where the ray leaves the layer, and

Δd is the thickness of the layer.

Some of these quantities are illustrated in Figure 3-1.

A summation over the layers involved produces the horizontal range and travel time for a ray path. In a non-refractive

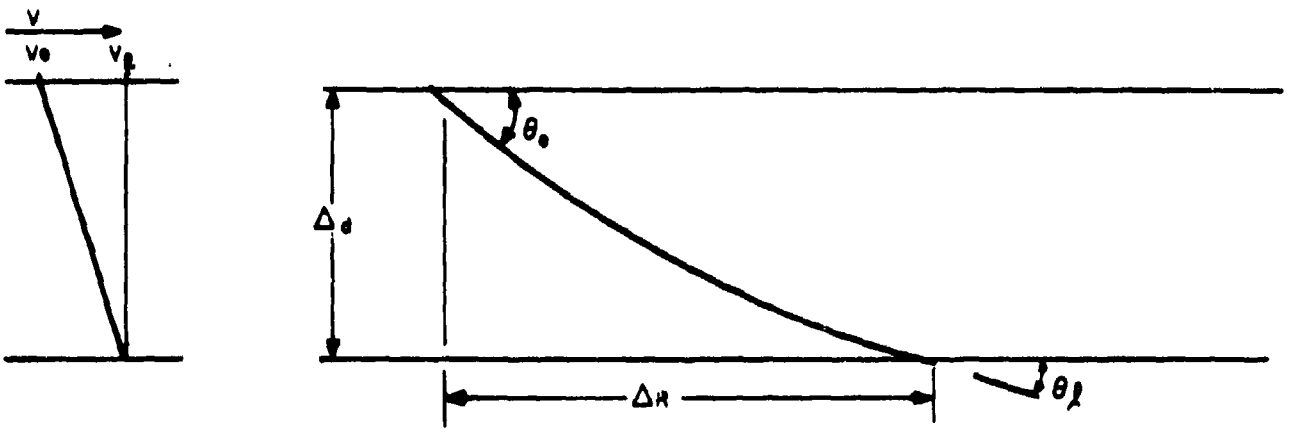

FIGURE 3-1. RAY PATH IN LAYER WITH CONSTANT VELOCITY GRADIENT

medium, the intensity at a point far from the source obeys the inverse square law: $I = I_o/r^2$. The analogue of the inverse square law for the refractive medium is the spreading loss factor. For a ray bundle travelling through a series of refractive layers, it is given by:

$$k_p = \frac{\cos\theta_o}{R\left|\frac{dR}{d\theta_o} \sin\theta_p\right|} \qquad (5)$$

where:

k_p is defined as the ratio of the sound intensity at a point p to the source intensity referenced to one yard,

R is the total horizontal range $(R = \sum_i R_i)$,

θ_o is the depression angle of the ray at the source, and

θ_p is the depression angle of the ray at point p.

The reader is directed to references 2 through 4 for the derivations and explanations of the above relationships.

4. Bottom Loss (Specular Reflections)

There are currently two semi-empirical equations used for the calculation of the specular reflection coefficient. The first one is based on a theoretical two-layer model for an absorbing bottom as reported by Mackenzie in Reference 5. The formula has been modified by the addition of some curve fitting parameters, enabling a satisfactory fit to the modified AMOS bottom loss data (Reference 6). For oceanographic areas which are adequately described by the two-layer model, the free parameters may be suppressed, leaving the theoretical expression.

The bottom loss equation, for the specular reflection coefficient, r, is

$$r = \left[\frac{(T-PQ \sin\theta)^2 + S^2}{(T+PQ \sin\theta)^2 + S^2}\right]\left(\frac{f}{C_1}\right) C_2(1-C_3\theta) \qquad (6)$$

where:

$$T^2 = (A-B)/2,$$

$$S^2 = (A+B)/2,$$

$$A = (B^2+4b^2)^{1/2},$$

$$B = P^2 \cos^2\theta - 1 + b^2, \text{ and}$$

$$b = b_o f^e.$$

Here,

P is the longitudinal velocity ratio (bottom/water),

Q is the density ratio (bottom/water),

b is related to the absorption coefficient of the bottom,

f is the frequency in cps, and

C_1, C_2, C_3, b_o and e are curve fitting constants.

For example, the constants used to fit the AMOS data are:

P = 1.025	C_1 = 3500 cps
Q = 1.2634	C_2 = 1.315
b_o = 0.0381	C_3 = -5.04
e = 0.0	

An alternative bottom loss expression is due to Dr. W. Watson of NEL:

$$N_B = \left[6 + 22(p-0.27) + 10 \log f_{kHz}\right] \times \tanh\left[\left(\frac{p}{0.24}\right)\left(\frac{\theta}{57.3}\right) + \left(1 - \frac{p}{0.24}{12.5}\right)\left(\frac{\theta}{90}\right)^2\right], \quad f_{kHz} \geq 1 \tag{7}$$

where:

N_B is expressed in db.

p is the porosity,

f_{kHz} is the frequency in kHz and

θ is the grazing angle of incidence in degrees.

5. Surface Loss (Specular Reflection)

There is insufficient information in the current literature to allow a reliable estimate of the surface reflection coefficient at the frequencies used in bottom-bounce sonars. References 26, 7, 8 and 9 indicate that, because of the large impedance mismatch between water and air, the surface reflection coefficient is close to unity. Although the contributions of these effects are not well-known, the surface can affect the signal through the following mechanisms:*

1. It can scatter energy out of the ray bundle. (Reference 26 indicates that energy may leave the surface channel by reflection from wave facets).

2. It can absorb energy from the signal (through the action of near-surface trapped air bubbles).

3. It can degrade the phase coherence along the wavefront, since the signal is reflected from randomly oriented facets of the surface. For a highly directional sonar, the full gain of the sonar could be lost for a signal propagating over a surface reflected path (as an upper limit). This coherence loss applies only to the echo; reverberation is generally assumed to be an incoherent process, so the reverberation intensity is not changed by a loss in signal coherence.

When estimating sonar performance in the bottom bounce mode, only a single path to the target is currently considered. This should provide a conservative estimate of the sonar's potential performance (since it implies a surface reflection coefficient equal to zero.

B. SCATTERING

1. Bottom Scattering (Non-specular reflections)

The bottom scattering coefficient μ_b is assumed to obey a generalized Lambert's Law expression:

$$\mu_b = \mu_{bo} (\cos \theta_i \cos\theta_s)^m \cos^n)$$

*See also References 34 - 37.

where

μ_{bo} is a constant of the diffusing surface,

$\cos \theta_i$ is the incident direction cosine with the normal to the surface,

$\cos \theta_s$ is the scattering direction cosine with the surface normal,

γ is the azimuthal angle between the incident and scattering directions, and m & n are curve-fitting constants, chosen so that the expression agrees with experimental results. (Isotropic scattering corresponds to m=n=0)

2. Sea Surface Scattering

Very few experiments have been reported dealing with the spatial dependence of non-specular reflection from the sea surface*. At present, a $\cos^n \gamma$ azimuthal dependence will be assumed, as in bottom scattering, to represent experimental data when it becomes available. An extension of the results for reciprocal ray paths is noted below. Modifications will be made as further experimental evidence becomes available. The equations for the sea surface scattering coefficient μ_s are based on the experimental work reported by Chapman, et al, in References 7 & 8, for the intermediate and large grazing angles over reciprocal ray paths. The equations are given below.

$$\mu_s = \mu_{se} + \mu_{sc} \tag{8}$$

where μ_{se} is based on Eckart's work and is given by

$$\mu_{se} = (8\pi\alpha^2)^{-1} \times 10^{-0.217\alpha^{-2}\cot^2\theta} \tag{9}$$

where

$$\alpha^2 = 0.003 + 0.00263W$$

and μ_{sc} is based on an "eyeball" fit to the corrected* Chapman and Harris data and it is given by

*See Reference 37.

$$\mu_{sc} = 10^{-(2.7 \log_{10}\beta + 1.16)} \times \left(\frac{\theta}{30}\right)^{0.33\beta} \qquad (10)$$

where

$$\beta = 158\ (Wf^{1/3})^{-0.58}$$

In the above equations,

W is the wind speed in knots,

θ is some combination of the incident and scattered grazing angles (θ_i and θ_s, respectively) chosen to represent experimental data $\left(\text{e.g. } \theta = \frac{\theta_1 + \theta_2}{2} \text{ ; or } \theta = \sqrt{\theta_i \theta_s}\right)$, and

f is the frequency in Hertz.

3. Deep Scattering Layer

Volume reverberation at the frequencies used in bottom bounce sonar is due primarily to fish with resonant or near-resonant air bladders. For any given location and time, these scatterers are generally confined to a relatively narrow depth interval. They may be treated as an equivalent scattering layer, commonly referred to as the deep scattering layer (DSL). The statistics of the low frequency DSL are currently under investigation by various Navy laboratories, but, at present, are not well known. Qualitative discussions of the DSL appear in References 11 to 16; most of the quantitative data for the bottom bounce frequency range is contained in References 7, 17, 18, and 38. Further, reverberation from the deep scattering layer is due to scattering from biological material with effective dimensions less than a wavelength and is generally considered to be isotropic.

SECTION IV

CONFORMAL/PLANAR ARRAY CONSIDERATIONS

A. THE PATTERN FUNCTION

The exact expressions for the pressure pattern for a rectangular array of uniformly driven point sources is derived from basic principles. Then adjustments are made to account for the effects of individual element directivity and for the effect of a finite baffle.

In the most general case, the pattern function (V) is given by:

$$V = \int_{\text{all space}} dV_o \frac{\rho(\vec{R}_o)}{R_o} e^{i(\vec{k}-\vec{k}_o)\cdot\vec{R}_o}$$

where: $\vec{k} = 2\pi/\lambda\ \hat{P}$, ($\hat{P}$ a unit vector in the observation direction),

$\vec{k}_o = 2\pi/\lambda\ \hat{P}_o$, ($\hat{P}_o$ a unit vector in the pointing direction)

$\vec{R}_o$ is the vector to the source point, and $\rho(\vec{R}_o)$ is the source velocity distribution. Since the pattern is of interest only in the far field, the vector $\vec{R}_o$ is written $\vec{R}_o = \vec{R} + \vec{r}$. In the far field, $R \gg r$, so that r need be retained only as a phase factor, allowing

$$V = \frac{e^{i(\vec{k}-\vec{k}_o)\cdot\vec{R}}}{R} \int_{\text{all space}} dV_o\ \rho(\vec{R}_o) e^{i(\vec{k}-\vec{k}_o)\cdot\vec{r}}$$

When all the transducers are driven with uniform velocity, the source velocity distribution is $\rho(\vec{R}_o) = V_o \sum_{j=1}^{N} \delta(\vec{R}_o - \vec{R}_j)$, in the approximation where the transducers may be considered as point sources. The volume integration over the Dirac functionals reduces the pattern function to a sum of exponentials.

Starting with the simple case of a line array of n uniformly driven point sources, spaced a distance, d, apart, the

pattern V is given by:

$$V = V_o \sum_{n=1}^{N} e^{inz}$$

where $z = kd(\cos\psi - \cos\psi_o)$, and
$k = 2\pi/\lambda$ is the wave number.

For a line array, the array axis forms the symmetry axis of the pattern. ψ is the angle formed by the direction of interest with the line of the array (as illustrated in Figure 4-1). Because of the symmetry of the pattern, ψ may be specified by the half-angle of the cone generated by the spatial direction and the array axis. Alternatively, with a view toward generalizing the definition of ψ for a rectangular array, $\cos\psi$ is the direction cosine of the spatial direction with respect to the line of the array.

The pattern is a geometric series with the sum:

$$V = V_{oe}^{iz}\left(\frac{1-e^{inz}}{1-e^{iz}}\right) = V_o e^{iz} e^{inz/2} e^{-iz/2}\left(\frac{e^{inz/2}-e^{-inz/2}}{e^{iz/2}-e^{-iz/2}}\right)$$

which is now a familiar form. We have, finally,

$$V = V_o e^{(iz/2)(n+1)} \frac{\sin nz/2}{\sin z/2}$$

which is the unnormalized pattern for a line of point sources.

B. SHADING THE ARRAY

The above discussion holds only if the elements of the array are driven with uniform velocity. The shape of the pattern, may be altered by driving the array non-uniform velocity distribution. A common application involves controlling the velocity distribution ("shading the array") in a special fashion to reduce the side-lobe level, at the expense of broadening the main beam. To model this (or other) velocity distribution without having to evaluate the summation for V explicitly, the array is considered

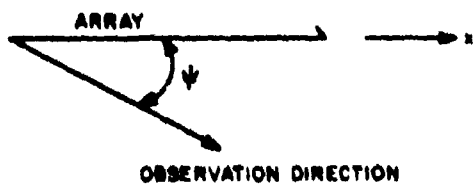

FIGURE 4-1. COORDINATES FOR A LINE ARRAY

to be composite, as shown in Figure 4-2.

In Figure 4-2, the δ_j's measure the displacement of the sub-arrays from the sub-array that represents the uniform velocity distribution (subscript "o"). The amplitude of each sub-array is denoted by the V_j. The velocity distribution is approximated by superimposing several sub-arrays so that the velocities of the sub-arrays, at any point along the array, add to the desired velocity.

It follows that the pattern from the shaded (composite) is given by the superposition of the patterns from the sub-arrays.

$$V = \sum_{j=o}^{J} V_{je}^{(iz/2)(n_j+1)} \frac{\sin n_j z/2}{\sin z/2} e^{ik\delta_j z/d}.$$

Consequently, the unnormalized pattern function for a shaded line array, composed of J sub-arrays, is given by

$$V = \frac{e^{iz/2}}{\sin z/2} \sum_{j=o}^{J} V_{je}^{iz(n_j/2 + K_j)} \sin(n_j z/2)$$

where the j^{th} sub-array starts with the element K_j (numbered from the left end).

Normalization is afforded by:

$$V_N = V\ (z=0) = \sum_{j=o}^{J} V_j/n_j$$

C. PATTERN FOR A RECTANGULAR ARRAY

The above discussion has been for a line array. The extension of these results to a rectangular array makes use of the well-known Product Theorem. The pattern of a rectangular array of uniformly driven, equi-spaced elements may be obtained by multiplying the pattern of the line array composed of one row of the elements of the rectangular array by the pattern of the line array composed of one column of the elements.

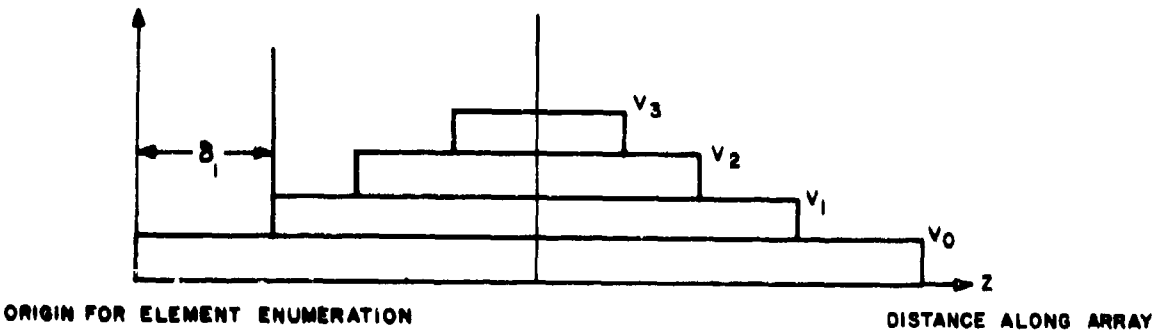

FIGURE 4-2. APPROXIMATE VELOCITY DISTRIBUTION FOR A SHADED LINE ARRAY

The Product Theorem is based on

$$e^{ik\cdot r} = e^{ik_x r_x} \cdot e^{ik_y r_y} \cdot e^{ik_z r_z} = e^{ikr_x} \cdot e^{ikr_y} \cdot e^{ikr_z}$$

The height and length patterns (of the line arrays referred to above) are formed separately. Ignoring the phase angle which lacks physical significance, the pattern of a uniformly driven, uniformly-spaced rectangular array (the length and height spacing may be different) is given by $V = V_L \cdot V_H$, with V_L and V_H computed as described above.

D. COMPUTING THE DIRECTION COSINES

The preceding discussion used direction cosines with respect to the array to define the cosines appearing in the expression $z = kd(\cos\psi - \cos\psi_o)$. The arguments for the length and height patterns are defined in terms of a coordinate system relative to the array. In practice, one is concerned with sonar coordinates, with depression angle measured positively above the horizontal, and azimuth ϕ measured from the ship's heading. This is illustrated in Figure 4-3.

The direction cosines relative to the array are obtained from the spatial direction cosines (defined relative to sonar coordinates) by a rotation of coordinates using the Euler angles defined as follows: The yaw angle Y is defined in the same manner as the azimuth angle. The roll angle R is taken as denoting rotation about the ship's longitudinal axis, and the pitch angle P, as measuring rotation about the ship's transverse axis.

The rotation of coordinates is accomplished by a matrix multiplication: $\vec{z} = \underline{\underline{A}} \cdot \vec{c}$,

where $\vec{c}$ is the vector of spatial direction cosines.

$$\vec{c} = \begin{pmatrix} \cos\theta \cos\phi \\ \cos\theta \sin\phi \\ \sin\theta \end{pmatrix}$$

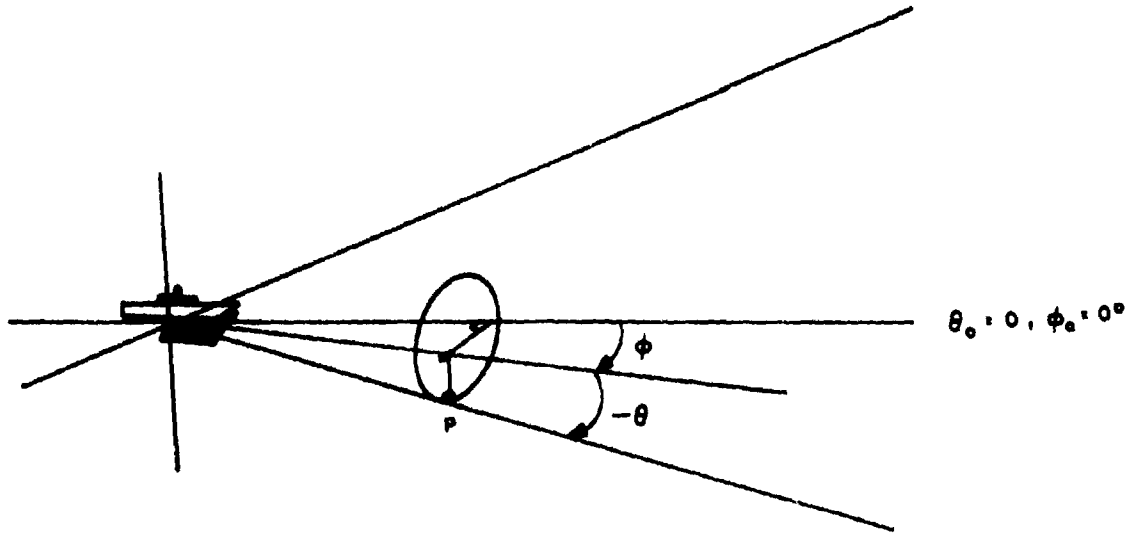

FIGURE 4-3. TRG SONAR COORDINATES

Combining the rotations,

$$\underline{\underline{A}} = \begin{pmatrix} \cos P \cos Y - \cos R \sin Y \sin P & \cos P \sin Y + \cos R \sin Y \cos P & \sin P \sin R \\ -\sin P \cos Y - \cos R \sin Y \cos P & -\sin P \sin Y + \cos R \cos Y \cos P & \cos P \sin R \\ \sin R \sin Y & -\sin R \cos Y & \cos R \end{pmatrix}$$

where

R= roll angle
Y= yaw angle
P= pitch angle

As an illustration, the calculation of the pressure pattern for an array with no pitch and yaw, with a roll angle $R = -\theta_T$ is shown below. (This is the pattern function presently used at TRG for the C/P array calculations).

Expanding $\underline{z} = \underline{\underline{A}}\underline{c}$, we have:

$$\begin{pmatrix} \cos\theta \cos\phi \\ \cos\theta_T \cos\theta \sin\phi - \sin\theta_T \sin\theta \\ \sin\theta_T \cos\theta \sin\phi + \cos\theta_T \sin\theta \end{pmatrix} = \begin{pmatrix} 1 & 0 & 0 \\ 0 & \cos\theta_T & -\sin\theta_T \\ 0 & \sin\theta_T & \cos\theta_T \end{pmatrix} \begin{pmatrix} \cos\theta\cos\phi \\ \cos\theta\sin\phi \\ \sin\theta \end{pmatrix}$$

Taking the first and third components of the $\vec{c}$ vector as z_L and z_H,

$$V = \frac{\sin\left[\frac{n_L \pi d_L}{\lambda}(\cos\theta\cos\phi - \cos\theta_o \cos\phi_o)\right]}{\sin\left[\frac{\pi d_L}{\lambda}(\cos\theta\cos\phi - \cos\theta_o \cos\phi_o)\right]} \times$$

$$\frac{\sin\left[\frac{n_H \pi d_H}{\lambda}\left(\cos\theta_T(\sin\theta - \sin\theta_o) + \sin\theta_T(\cos\theta\sin\phi - \cos\theta_o \sin\phi_o)\right)\right]}{\sin\left[\frac{\pi d_H}{\lambda}\left((\cos\theta_T(\sin\theta - \sin\theta_o) + \sin\theta_T(\cos\theta\sin\phi - \cos\theta_o \sin\phi_o)\right)\right]}$$

after introducing the pointing direction (zero subscript). This expression is consistent with the expression given in Reference 24.

E. INDIVIDUAL ELEMENT DIRECTIVITY FACTOR

The above calculations make the assumption that the C/P array is composed of point sources. The directivity of the pistons of finite diameter may be taken into account by the factor $Q = J_1(ka \sin(w)) / ka \sin(w)$

where J_1 denotes the first order cylindrical Bessel function,

k is the wave number, as before,
a is the piston radius, and
$w = \cos^{-1}(z_2)$

(z_2 is the second component of the z vector introduced above, the direction cosine with respect to the normal of the array).

Noting that $\frac{\sin(\cos^{-1}(t))}{\sqrt{1-t^2}} = U_o(t)$, the zero order associated Tchebycheff polynomial, the individual element directivity factor can be written in the computationally convenient form: $Q = J_1\left(ka\sqrt{1-z_2^2}\right) \Big/ ka\sqrt{1-z_2^2}$ (noting $U_o(t) = 1$)

(For square elements, a similar expression may be used).

F. FINITE BAFFLE EFFECT

The above expressions are for an array in a free acoustic field. As mounted on a ship, the transducers are in a rigid baffle (after resonant stiffening) which has the effect of doubling the pressure pattern (since radiation is restricted to a half-space). Diffraction is a further effect of the finite baffle. The form of the expression for the baffle diffraction has been reported in several TRG reports under this contract. Reference 28 developed equations, in terms of the Fresnel integrals, for the finite baffle effect for baffles large with respect to a wavelength. Reference 29 compared the patterns of an array on a cylinder with the pattern of an array on a plane and found that the

effects of curvature are small. A computationally convenient form of the finite baffle diffraction expression is a subject for further investigation.

G. ARRAY SELF-NOISE

Derived from at-sea measurements (see Reference 20), the noise level used in systems calculations includes flow noise, machinery noise, vibration, and ambient sea noise. Adding element outputs in an array increases noise and signal at different rates due to an averaging of the random noise over the many elements of the C/P array while the non-stochastic echo adds coherently. Accordingly, the array gain against noise is proportional to the number of elements in the array.

Array Gain = 10 $\log_{10}$ (number of elements in array).

SECTION V

DETERMINATION OF THE ECHO LEVEL

The echo level is the acoustic intensity at the receiver due to the reflection of energy from the target. The basic process concerns the flow of energy from a point "A" in a refractive medium to a point "B". The bistatic echo is developed in two stages. The energy produced at the source is transmitted over some ray path to the target. Then a fraction of this energy, given by the target strength, is directed over another ray path to the receiver. A knowledge of these ray paths permits the calculation of the propagation loss, the deviation losses due to the array patterns, and the insonification, all of which are considered below. Finally, these results are combined with the target strength to yield the echo level.

In general, several types of propagation paths may exist between the source and the target, and between the target and receiver. A given transmission and reception path pair will create an echo at the time t'. Other combinations of paths will deliver the echo at some different time t'', and may be considered separately. To simplify the following discussion, results are presented for any particular pair of ray paths. Since the nature of the echo level is independent of the details of the ray paths, the discussion holds for any combination of transmission and reception ray paths. If multiple paths exist such that the respective echoes overlap in time, then the observed echo is a summation of each of the contributing echoes. All processes considered below have this implied summation over all transmission-reception path pairs. (This results in a considerable simplification of the equations; supplying the summation over all ray paths is a simple operation.)

A. RAY TRACING (FINDING THE RELEVANT RAY PATHS)

This section is concerned with the determination of the source depression angles for the ray path starting at the point "A" and ending at the point "B" in a refractive medium. The transmission and reception paths, specified by their depression angles, are found as described below.

Section III spells out the ray-tracing equation for an ocean modelled by a refractive medium consisting of horizontal layers with a constant velocity gradient. For the purposes of systems calculations, the sound velocity is adequately represented as a function only of depth. While the details of the results below depend on this representation of the ocean, the conclusions and techniques are valid for any convenient representation of the velocity profile.

The technique of ray-tracing discussed in Section III allowed the calculation of the horizontal range traversed, given the source depression angle. The echo level computation requires the solution of the inverse problem: Given the horizontal range to the target, find the source angle of the ray that reaches the target. Since the formula for the horizontal range travelled by a ray, as a function of its source angle, does not allow inversion to yield an analytic expression, iterative techniques are used to find the source depression angle for the ray connecting points "A" to "B".

By their nature, iterative schemes require an initial estimate. For bottom-bounce ray paths, source angle estimates are derived from isovelocity considerations. Methods for developing estimates of source angles for direct paths are under development. A promising scheme obtains an initial estimate of the depression angle from a polynomial fit to sample points of the inverse $\theta(R)$. These estimates are refined by iterative techniques until the error is within satisfactory bounds.

B. PROPAGATION LOSSES FOR THE ECHO LEVEL

Once the above scheme is applied to find both the transmission and reception ray paths, the propagation losses (including attenuation, spreading losses, and losses on specular reflection from the boundaries) are computed as set forth in Section III.

For situations in which ray tracing is not valid, empirical formulae will be implemented. In shallow water, for example, ray tracing becomes impractical; the COLOSSUS formulae might be used in this instance. Special cases, where ray-tracing is not practical are handled separately and are not discussed in this report.

C. DEVIATION LOSS

The deviation loss is a measure of the amount a signal is diminished by the array pattern, relative to signals on the beam axis. As discussed in Section IV, the pattern is specified by two angle pairs (θ, ϕ), and (θ_o, ϕ_o). The pair with the subscript "o" refers to the steering (pointing) direction, and the other, to the observation direction. The ray inclination angle is fixed by the geometry and travel time constraints.

For reception, the observation azimuth is specified by the angle which yields the maximum echo level, denoted by ϕ_o^*. (This is realistic, since it yields the most probable target bearing, and is the bearing that operational systems will indicate.) For cylindrical sonars, the observation azimuth is simply ϕ_{ro} since there is no beam skewing. For C/P sonars, (unlike conventional cylindrical sonars) the most probable target bearing depends on the ray depression angle θ_r, itself a function of the range. (The azimuthal angle that yields the maximum echo level is given by $\phi_r^* = \phi_r^* \quad (\theta_r, \phi_r, \theta_{ro}, \phi_{ro})$, with θ, θ_{ro}, and ϕ_{ro} held constant.) An iterative technique, similar to the one described in Reference 24 will be used to find the azimuthal

angle which maximizes the receiving pattern for C/P sonars.

The pattern function is also dependent on the "pointing" angles (θ_o, ϕ_o). For reception, both the depression pointing angle θ_{or}, and the azimuthal pointing angle ϕ_{or} are fixed by the operator. This completes the specification of the reception pattern. The transmission pointing angles (θ_{ot}, ϕ_{ot}) also are decided upon in advance. For transmission, the observation azimuth is determined from purely geometric considerations.

D. THE INSONIFICATION

Insonification is defined at a point "A" as the energy flux through a differential area, normal to the ray path. The insonification process can be characterized by an effective pulse length and a peak intensity for each direction. This pulse length, a constant for a fixed depression angle, is chosen so that the product of the pulse length and intensity function describe the total energy flux transmitted in each direction. Propagation losses along the ray path from the source to point A are taken into account as described above.

When the source level depends upon the steering direction, the source intensity will be represented by a polynomial which passes through sample points (e.g. from a cavitation-limited source level computation, or experimental data). For a single transmitted pulse, the intensity function is simply the source intensity, modified by the transmitting pattern. When using the RDT mode, the calculation of the insonification is simplified by using the peak intensity at the point "A" and an effective pulse length to yield the total flux. Since the transmission depression steering angle is fixed by choice, the peak source intensity for a given observation direction depends only on the steering azimuth. An iterative technique locates the azimuthal beam that yields the peak intensity, allowing the complete specification of the insonification.

The peak intensity function (I_e) is given by:

$$I_e(\phi_t, \theta_t) = \max_{\phi_{ot}} \Big[\text{Source Intensity}(\theta_{ot}, \phi_{ot}) \cdot (\text{Transmitting Pattern } (\theta_{ot}, \phi_{ot}, \theta_t, \phi_t))\Big]$$

E. THE BISTATIC TARGET STRENGTH

The above specifies the calculation of the insonification and propagation losses. Only the target strength for non-reciprocal ray paths is needed to complete the echo level computation. Information on the target strength viewed by sonars using a receiver remote from the source is scanty. Available sources (See references 21 and 22), indicate that the target return is quite structured. Averaging over small solid angles to remove this fluctuation, a mean target strength, independent of the bistatic angle results (geometry is illustrated in Figure 5-1). This averaged target strength, ranging from 10 db dead on, to 20+ db for a broadside view, depends only on the aspect angle. The target strength represents the fraction of the energy incident on the target that is scattered to the receiver.

F. THE ECHO LEVEL

With the above computations completed, the echo level is given by:

ECHO LEVEL = SOURCE LEVEL
- DEVIATION LOSS (Transmission)
- PROPAGATION LOSS (Transmission path)
- PROPAGATION LOSS (Reception path)
- DEVIATION LOSS (Reception)
+ SIGNAL PROCESSING GAIN

(All quantities are expressed in db relative to some reference level 0).

The echo level calculations described above yield the maximum echo level that the system will obtain. If the average

echo level is desired, the azimuthal deviation losses must be accounted for; these depend on the beam spacings used in transmission and reception. (Note that the beam spacings for these two modes are determined independently. See Reference 19 for further discussion concerning the selection of RDT beam spacings.)

SECTION VI

BOUNDARY REVERBERATION

The reverberation from the horizontal ocean boundaries and biological scatterers that arrives at the receiver at the time of the echo competes with the echo. Specular reflections from these boundaries have discrete travel times to the receiver, and, generally, are not likely to interfere with echoes. Non-specular reflections from the surface and bottom were characterized in Section III. The discussion of the deep-scattering layer (DSL) in Section III indicates that the biological scatterers, at the frequencies of interest for a C/P sonar, tend to congregate in well-defined layers. For the purpose of estimating the energy scattered by the DSL to the receiver, the scatterers may be lumped into discrete layers. (This corresponds to a numerical integration over the scattering region in depth.)

Accordingly, the three forms of reverberation may be treated by a general discussion of reverberation from a plane boundary. The contributing area on the surface under consideration is determined by simultaneous application of temporal and spatial constraints. With the contributing area defined, the differential expression for reverberation is integrated to yield the reverberation level for the surface. A sum over all surfaces (bottom, surface, and DSL), and over all ray paths to and from these surfaces produces the total reverberation level. In a discussion of boundary reverberation, it is convenient to put aside a consideration of the combinations of ray paths linking the source, reverberating surface, and the receiver, and concentrate on the essence of boundary reverberation. Since all three types of boundary reverberation are conceptually the same, the following discussion of boundary reverberation can hold for all reverberating surfaces, for any combination of ray paths from the source to the reverberating area, and from the reverberating area to the receiver.

A. SPECIFICATION OF THE CONTRIBUTING ANNULUS

To compete with the echo, the energy scattered from the reverberating surface must arrive at the time of the echo (T_e). The ray path associated with the reverberation must start at the source, strike the reverberating surface, and end at the receiver. Vector notation will be used wherever practical in the following, to point out that the results are independent of the choice of the coordinate system. Parameters associated with the transmission path are identified by the subscript "t"; those related to the reception path, by a subscript "r". This leads to the set of equations:

$$T_t + T_r = T_e$$

$$\vec{\rho}_t + \vec{\rho}_r = \vec{s}_o$$

where $\vec{s}_o$ is the vector between the source and receiver, $\vec{\rho}_{(t/r)}$ is the vector between the (source/receiver) and the point of contact of the reverberating ray path with the surface, and T denotes travel time.

The simultaneous solution of these equations proceeds by an iterative method. (Both travel time and range are functions of the source and receiver angles.) The Newton iteration, operating on both depression angles, is convenient once an initial estimate is gotten from a solution of the range equation for a point on the reverberating boundary on a line with the source and receiver. An initial estimate of the depression angles is obtained from an isovelocity solution chosen to give a total travel time equal to the echo time. In general, these ray paths will not meet; holding one source angle fixed, the other is varied so that the ray paths meet on the reverberating surface. This, however, yields a travel time different from the echo time. Then, the time constraint equation is modified to cancel the difference in the travel times. The iteration is continued until the travel time and range error (a vector) are within satisfactory limits.

An isovelocity ocean restricts the reverberating area to an annulus having the shape of a cross-section of an ellipse. The ellipse, with the source and receiver as foci, is defined by the echo time. The wall thickness width of the annulus is determined by the pulse length. (See figure 6-1) In the usual case where the travel times of interest greatly exceed the pulse length, the wall of reverberating annulus is quite thin. Since the insonification is nearly constant across the narrow width, the integration of the differential reverberation may be reduced to a contour integration. With this assumption, one of the integrals of the surface integration is done implicitly. The surface integral reduces to a line integral over the reverberating contour. Although the results which follow do not depend on the reverberating annulus having the shape of an ellipse, the isovelocity geometry gives a useful insight. While the refractive ocean will change the shape of the reverberating annulus somewhat, the characteristics of the reverberation geometry are not seriously altered.

Once a solution to the range and travel time equations is established for a point on the line connecting source and receiver (this line is the projection of $\vec{s}_o$ onto the reverberating plane), the contributing contour is traced out by the following scheme. (The technique to find a point on the connecting line is the same as the one presently used in TRG's monostatic calculations.) Figure 6-1 illustrates the geometry.

1. With ϕ_t and ϕ_r set to the source and receiver mutual relative bearings, the resulting 2 x 2 set of equations for horizontal range and travel time is solved for θ_t and θ_r, as for the monostatic case, by the iterative scheme outlined above.

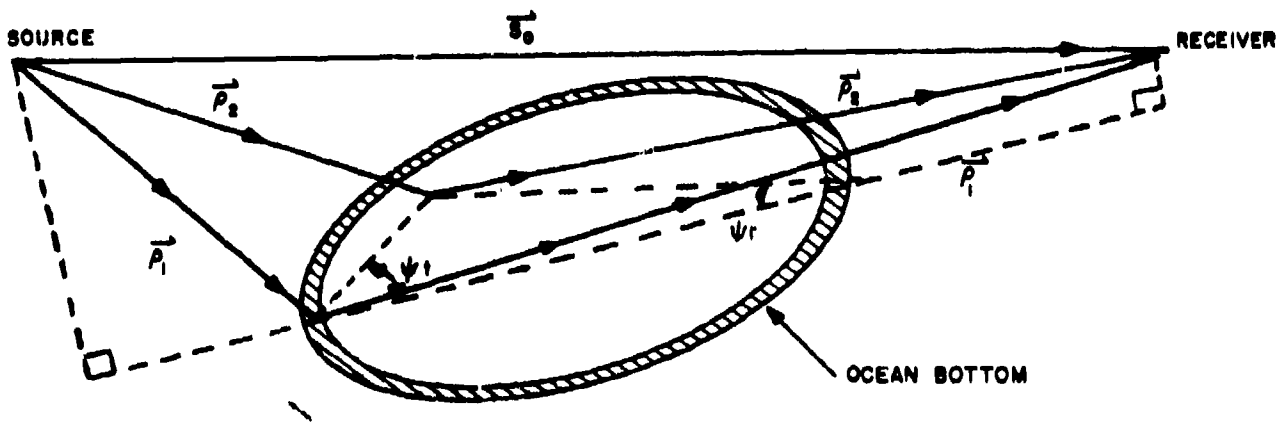

FIGURE 6-1. SIMPLIFIED REPRESENTATION OF BISTATIC REVERBERATION GEOMETRY (THE REVERBERATING AREA IS SHADED).

2. The transmission depression angle (θ_t) is incremented by a small $\Delta\theta_t$. The time constraint gives $\Delta\theta_r$ from:

$$\left.\frac{\partial T_t}{\partial \theta_t}\right|_{\theta_t} \Delta\theta_t + \left.\frac{\partial T_r}{\partial \theta_r}\right|_{\theta_r} \Delta\theta_r = 0 = \Delta T$$

so that

$$\Delta\theta_r = -\frac{\left.\frac{\partial T}{\partial \theta_t}\right|_{\theta_t}}{\left.\frac{\partial T}{\partial \theta_r}\right|_{\theta_r}} \Delta\theta t$$

3. Given the depression angles, the transmission and reception azimuths are found so that the one-way vector ranges meet at a point on the contributing annulus. Note that the reception depression angle is chosen for θ_t fixed to satisfy the travel time constraint. Since the azimuths are defined with respect to the sonar coordinate system, it becomes necessary to resort to a coordinate system to calculate the azimuth angles. Let $\hat{n}_{t/r}$ denote the unit vector in the direction of the source/receiver, and $\hat{z}$ be the unit vector in the vertical. Now, $\vec{\rho}' = \vec{\rho} - \hat{z}(\vec{\rho}\cdot\hat{z})$ is a vector with components only in the horizontal plane. (Unsubscripted vectors stand for both transmission and reception.) The azimuthal angles are found by noting that cos ϕ is the direction cosine of the $\vec{\rho}'$ vector with the heading unit vector.

$$\cos\phi = \frac{\vec{\rho}'\cdot\hat{h}}{|\vec{\rho}'|}$$

5. At any point on the reverberating contour, the width of the annulus is found from:

$\Delta R = \vec{\rho}(T) - \vec{\rho}(T-\tau)$, with τ standing for the pulse length.

B. THE DIFFERENTIAL REVERBERATION INTENSITY

The reverberating area, defined for a particular set of transmission and reception paths, is the locus of points such that the paths from the source to the surface and from the surface to the receiver have a travel time equal to the echo time (within a few pulse lengths). The differential reverberation calculation is conceptually the same as the echo calculation, when the target is taken to be a differential area on the reverberating boundary. The scattering coefficient μ, a function of the direction cosines with respect to the normal to the surface is chosen to conform to observed data for the surface of interest.

Then, the general expression for the differential reverberation intensity due to a reverberating boundary is:

$$dI_r \quad \mu(\theta'_t, \theta'_r) K_t(\theta'_t) K_r(\theta'_r) I_o(\theta_t, \phi) V_r(\theta_r, \phi) dA$$

where

μ is the scattering coefficient per unit area,

θ' is a grazing angle at the boundary

γ is azimuthal angle between the incident and scattering directions

K is the ray bundle spreading loss factor

V_r is the receiving intensity function

I_o is the transmitting source intensity function, which for a single pulse is given by

$$I_o(\theta_t, \phi) \quad I_o V_T(\theta_t, \phi)$$

where (θ_{ot}, ϕ_{ot}) is fixed,

and for RDT is given by

$$I_o(\theta_t, \phi) \quad \max_{\phi_{ot}} \left[I_o(\phi_{ot}) V_T(\phi_{ot}, \theta_t, \phi) \right]$$

where (θ_{ot}) is fixed.

where :

V_T is the transmitting intensity pattern function,
I_o is the source intensity function, and
dA is the differential area of concern.

The selection of a coordinate system, useful for the numerical integration of the reverberation, depends upon the character of the insonification of the reverberating area. This is under investigation.

C. THE NUMERICAL INTEGRATION FOR THE REVERBERATION

Since a closed-form expression for the differential reverberation intensity has not been found for the general case, a numerical integration over the contour is used to calculate the reverberation. Previous experience with numerical integrations of this nature indicates that adaptive schemes are not very helpful; they seem to require a number of sample points approximately equal to twice the number of peaks in the insonification of the annulus. A straight-forward scheme, based on the upper and lower sums that bound the Riemann integral, appears promising. This scheme has the advantage that a truncation error estimate is available from a comparison of the upper and lower sums.

Upon examination of the bistatic insonification of the reverberating areas, an analytic approximation, patterned after the one detailed for the monostatic case in Appendix A of Reference 24 may be developed to replace the numerical integration wherever possible.

D. ECHO-TO-BACKGROUND RATIO

With the calcultaions presented above completed, the echo-to-background ratio is easily computed from:
E/B = Echo Level - (Total Reverberation + Self-Noise). The estimation of self-noise is described in Section IV, the echo-level, in Section V, and the reverberation (summed over all types

and orders), in this section. The noise and reverberation components are assumed to have random phases and their powers added to obtain total background level. These echo-to-background ratio calculations provide the means for a study of bistatic echo ranging. A full understanding of the nature of echo ranging with systems using a remote receiver may lead to more fruitful employment of present sonar systems, and provide a guide for the design of future ones.

SECTION VII

REFERENCES

1. A. Novick, Estimation of Performance of Sonar System (U), TRG-142-TN-64-9, TRG, Inc., dated May 1965. CONFIDENTIAL

2. Physics of Sound in the Sea, Part I: Transmission, NDRC Summary Technical Reports.

3. E. Eby and T. Einstein, The Computation of Spreading Loss in Layered Media, USL Report No. 609, dated April 1964.

4. A. Novick, "Derivative of Travel Time with Respect to Source Angle for a Layer of Constant-Velocity Gradient," Journal of the Acoustical Society of America, Vol. 36, No. 6.

5. K. V. Mackenzie, "Long-Range Shallow-Water Transmission," Journal of Underwater Acoustics, Vol. 7, No. 4. CONFIDENTIAL

6. T.G. Bell, "A Theoretical Comparison of the Bottom-Bounce Capabilities of AN/SQS-23 Versus AN/SQS-26 Surface Ship Sonars," USL Report No. 449, dated October 1959. CONFIDENTIAL

7. R. P. Chapman and J. H. Harris, "Surface Backscattering Strengths Measured with Explosive Sound Sources," Journal of the Acoustical Society of America, Vol. 34, No. 10.

8. R. P. Chapman and H.D Scott, "Surface Backscattering Strengths over an Extended Range of Frequencies and Grazing Angles," Journal of the Acoustical Society of America, Vol. 36, No. 9.

9. C. Eckart, "The Scattering of Sound from the Sea Surface," Journal of the Acoustical Society of America, Vol. 25, No. 3.

10. C. Cox and W. Munk, "Measurement of the Roughness of the Sea Surface from Photographs of the Sun's Glitter," Journal of the Optical Society of America, Vol. 44, No. 11.

11. J. B. Hersey and R. H. Backus, "Sound Scattering by Marine Organisms," in The Sea, Volume I, by M. N. Hill, General Editor. Interscience Publishers, New York, 1962.

12. G. L. Clarke and E. J. Denton, "Light and Animal Life," in The Sea, Volume I, by M.N. Hill, General Editor. Interscience Publishers, New York 1962.

13. J. Y. Costeau, The Living Sea, Harper and Row, New York, 1963.

14. R. Carson, The Sea Around Us, Oxford University Press, New York, 1961.

15. J. Fraser, Nature Adrift, Dufour Editions, England, 1962.

16. R. S. Dietz, "The Sea's Deep Scattering Layers," Scientific American, August 1962.

17. J. R. Marshall and R. P. Chapman, "Reverberation from a Deep Scattering Layer Measured with Explosive Sound Sources," Journal of the Acoustical Society of America, Vol. 36, No. 1.

18. G. H. Bowers, Jr.,"Volume Reverberation from Deep Scattering Layers," Report No. MED-65-1001, AVCO Marine Electronics Office, dated October 1965.

19. A. Novick, On the Choice of Beam Spacing in Rotational Directional Transmission, Report WP11-1-43003, TRG, Inc., dated April 1966.

20. S. Gardner, Noise and Vibration Measurements on the USS Brownson (DD868), TRG-142-TN-64-4, TRG, Inc., dated May 1964. CONFIDENTIAL

21. A. Novick, Note on the Selection of an Array Tilt for the C/P Sonar, Report No. 023-TM-66-8, TRG, Inc., dated March 1966.

22. "U.S Navy Journal of Underwater Acoustics," Vol. 10, No. 1, January 1960, p63-74. Article: "Target Strenght-An Addendum to Part II of the Summary of Underwater Acoustic Data," R. J. Urich and A.W. Pryce.

23. "USN Journal of Underwater Acoustics," Vol. 5, No. 1, January 1955. Article: "Sonar Echoes from a Scaled Model Submarine Hull," N.B. Tatge and R. D. Fay.

24. "Interim Report on Sonar Performance," A Novick and R. Seegal, Report No. 023-TM-66-16, Contract NObsr-93023.

25. "Further Results On Sound Scattering by the Sea Surface", H.W. Marsh and E.Y. Tkuo, Avco Marine Electronics Office, Contract N140(70024)76924B.

26. "Acoustic Reflection at the Sea Surface," R.H. Adlington J. Acoust. Soc. Am 35, 1834 (Nov. 1963)

27. "Intensity Reflections of Direct and Surface Reflected Signals Transmitted from a Deep Source", USNJUA 12, 41-48.

28. "The Far-Field Pattern of a Line Source on a Strip or Half-Plane", V Mangulis, Report No. 023-TM-65-24, Contract NObsr 93023.

29. "Comparison of the Far-Field Patterns of an Array on a Cylinder with an Array on a Plane", V. Mangulis, A. Kane, E. Paige, Report 023-TM-65-4, Contract NObsr 93023.

30. "Toward the Elimination of Ocean Environment Variations in Integrated Detection, Localization, and Attack Systems (U)," R.H. Mathes and L.C. Ricalzone, NRL Report 6247, May 3, 1965.

31. "1964 Annual Summary Progress Report on Underwater Target Classification (U)" General Dynamics/Electronics, Rochester, New York Contract No. Nonr 2646(00) NR No. 261-117.

32. "Operations Analysis by Sikorsky Aircraft", M.I. Nabel, Sikorsky Aircraft, Stratford, Conn. (Included as an appendix in reference 31.

33. "Volume Reverberation at a Receiver Located at a Distance from the Sound Source," A. McWilliams, USL Tech. Memo No. 1170-78-57 Sept. 11, 1957

34. "Sound Reflection and Scattering by the Ocean Boundaries," Avco Marine Electronics Office, New London, Conn., Dec. 1, 1963 AD C15918

35. "Diffraction by a Periodic Surface." I.A. Urasouskii "Soviet Physics - Acoustics" 10, 3, P287ff

36. "Coherent Reflection of Sound from an Ocean Surface Layer Containing Resonance Scatterers" U.P. Glotov and Yu. P. Lysanov "Soviet Physics - Acoustics " 10, 4, P360 ff.

37. "Experiments in the Spatial Correlation of the Amplitude and Phase Fluctuations of Acoustic Signals Reflected from a Rough Ocean Surface" E.P. Gulin and K.J. Malshev "Soviet Physics - Acoustics" 10, 4, P365 ff

38. "Scattering of Sound by Air Bladders of Fish in Deep Sound-Scattering Ocean Layers," I.B. Andreeva "Soviet Physics - Acoustics" 10, 1 pp7 ff.